BIOCHEMISTRY
including biophysical chemistry & molecular biology

Article

pubs.acs.org/biochemistry

Recognition of Double-Stranded RNA by Guanidine-Modified Peptide Nucleic Acids

Pankaj Gupta, Oluwatoyosi Muse, and Eriks Rozners*

Department of Chemistry, Binghamton University, The State University of New York, Binghamton, New York 13902, United States

Supporting Information

ABSTRACT: Double-helical RNA has become an attractive target for molecular recognition because many noncoding RNAs play important roles in the control of gene expression. Recently, we discovered that short peptide nucleic acids (PNA) bind strongly and sequence selectively to a homopurine tract of double-helical RNA via formation of a triple helix. Herein, we tested if the molecular recognition of RNA could be enhanced by α-guanidine modification of PNA. Our study was motivated by the discovery of Ly and co-workers that the guanidine modification greatly enhances the cellular delivery of PNA. Isothermal titration calorimetry showed that the guanidine-modified PNA (GPNA) had reduced affinity and sequence selectivity for triple-helical recognition of RNA. The data suggested that in contrast to unmodified PNA, which formed a 1:1 PNA−RNA triple helix, GPNA preferred a 2:1 GPNA−RNA triplex invasion complex. Nevertheless, promising results were obtained for recognition of biologically relevant double-helical RNA. Consistent with enhanced strand invasion ability, GPNA derived from D-arginine recognized the transactivation response element of HIV-1 with high affinity and sequence selectivity, presumably via Watson−Crick duplex formation. On the other hand, strong and sequence selective triple helices were formed by unmodified and nucelobase-modified PNA and the purine-rich strand of the bacterial A-site. These results suggest that appropriate chemical modifications of PNA may enhance molecular recognition of complex noncoding RNAs.

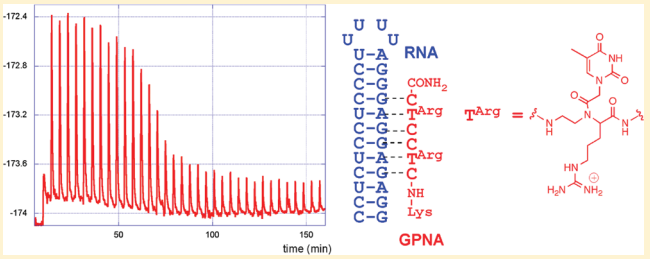

Recent discoveries that noncoding RNAs play important roles in the regulation of gene expression stimulate interest in molecular recognition of double-helical RNA. However, discovery of small molecules that recognize helical RNA structure and selectively modulate RNA's function has been a challenging and involved process.[1−3] The RNA helix has a relatively uniform and polar surface that presents little opportunity for hydrophobic shape selective recognition. On the other hand, binding to bulges and internal loops, which are the most common small molecule targets in RNA, is frustrated by the conformational flexibility of nonhelical RNA. Hydrogen bond-mediated sequence selective triple-helix formation could provide a straightforward and effective molecular recognition of double-helical RNA.[4] Surprisingly, triple helices involving the RNA duplex have been little studied. Modestly stable, all RNA triple helices are formed via parallel binding of a pyrimidine-rich third strand to a purine-rich strand of the double helix.[5−7] The molecular recognition of RNA's sequence occurs via the Hoogsteen hydrogen bonding between uridine and adenosine-uridine base pairs (Figure 1, U*A-U triplet) and between protonated cytidine and guanosine-cytidine base pairs (C*G-C triplet). In contrast to DNA, RNA does not form the pH-independent antiparallel triplex based on G*G-C, A*A-T, and T*A-T triplets.[7,8]

Practical applications of triple-helical recognition of nucleic acids are limited by (1) the low stability and slow formation of the triplex caused, at least in part, by electrostatic repulsion between the negatively charged phosphate backbones of the

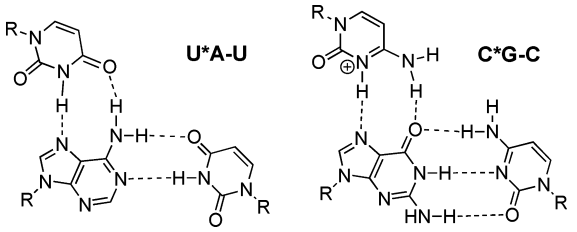

Figure 1. Triple-helical recognition of RNA via Hoogsteen base triplets.

double helix and the incoming third-strand oligonucleotide and (2) the requirement for long homopurine tracts, as only U*A-U and C*G-C triplets are used in the common triple-helical recognition. Recently, we discovered that short peptide nucleic acids (PNA)[9] recognized double-helical RNA via highly stable and sequence selective triple-helix formation.[10−12] PNA, as short as hexamers, formed triple helices with a RNA duplex faster and with higher affinity than with RNA as the third strand.[10] Furthermore, nucleobase modifications allowed recognition of isolated pyrimidine inversions in short polypurine tracts, thus expanding the potential of recognition to biologically relevant double-helical RNA, such as rRNA and

Received: October 12, 2011
Revised: December 6, 2011
Published: December 7, 2011

microRNAs.[12] These findings inspired a hypothesis that, because of the absence of a negatively charged backbone, PNA will be a superior candidate for triple-helical recognition of RNA and may overcome the limitations of natural oligonucleotides in triple-helical recognition. Interestingly, despite extensive studies of DNA–PNA triplexes,[13] binding of PNA to double-helical RNA had not been studied before our recent work.[10−12] Our results encouraged us to further explore the potential of chemically modified PNA in molecular recognition of double-helical RNA.

Despite the excellent chemical and biophysical properties, in vivo applications of unmodified PNA have been limited because of poor uptake by mammalian cells. Recent work on chemically modified PNA showed that the cellular delivery may be enhanced by attaching cationic cell-penetrating peptides.[14,15] Ly and co-workers[16−18] developed guanidine-modified PNA (GPNA, the backbone derived from arginine instead of glycine) that maintained strong and sequence selective binding to complementary single-stranded DNA and RNA and were efficiently taken up by several cell lines. The enhanced cellular uptake was attributed to the positively charged guanidine groups. We were interested in probing the potential of GPNA in molecular recognition of double-helical RNA. We envisioned that combining the high affinity and sequence selectivity of the PNA–RNA triplex, as observed in our recent studies,[10,12] with the cellular penetration of GPNA would pave the road for in vivo applications of sequence selective recognition of double-helical RNA. Herein we used isothermal titration calorimetry and fluorescence spectroscopy to study binding of GPNA to double-helical RNA. The results were further confirmed using circular dichroism (CD) spectroscopy and a gel mobility shift assay. We found that guanidine modification reduced the affinity and sequence selectivity of PNA with respect to complementary double-helical RNA. The binding stoichiometry increased to a 2:1 PNA–RNA complex, suggesting that the most likely mode of binding was a strand invasion triplex. While GPNA did not favor triple-helix formation, strong and sequence selective recognition of transactivation response element (TAR) RNA of HIV-1 was achieved using the GPNA derived from D-arginine in a strand invasion mode. Unmodified and nucleobase-modified[12] PNA also gave promising results for triple-helical recognition of bacterial A-site RNA.

EXPERIMENTAL PROCEDURES

Isothermal Titration Calorimetry. In a typical ITC experiment, an RNA hairpin solution (0.95 mL, 5.25 mM) in acetate buffer [100 mM sodium acetate and 1.0 mM EDTA (pH 5.5)] was titrated with a PNA solution (50 × 5 μL, 96 mM) using a Nano ITC G2 (TA Instruments) calorimeter. For full experimental details and data, see the Supporting Information. The titration data (Figures S1–S42 of the Supporting Information) were analyzed using NanoAnalyze (TA Instruments) using an independent model to obtain the fitting graph and thermodynamic binding data (Table S1 of the Supporting Information).

Fluorescence Spectroscopy. An HRP7 (TAR RNA model) solution (2 mL, 0.1 mM) in phosphate buffer [10 mM phosphate, 0.1 mM EDTA, and 1 mM $MgCl_2$ (pH 6.8)] was heated for 6 min in a 90 °C water bath and then snap-cooled by being immediately placed in an ice bath. The sample was placed in a 1 cm path length cuvette and equilibrated at 20 °C using a circulating water bath. The excitation wavelength was set to 305 nm; the emission wavelength was observed at 365 nm. The excitation and emission bandwidth was 10 nm. Titration of the PNA into TAR RNA was achieved via addition of 1–6 μL aliquots of concentrated PNA stock solutions to reach the required PNA concentration of 0.002–2 μM. After each addition of PNA, the mixture was stirred for 30 min before the fluorescence intensity was measured using a Shimadzu RF-5301pc spectrofluorometer. The data were analyzed by fitting (Figures S44–S50 of the Supporting Information) the change in fluorescence intensity to a single-site, two-state binding model as previously described.[19]

RESULTS

Our study started with modification of the synthetic route designed by Ly and co-workers[16,18] for preparing Fmoc-protected GPNA monomers that would be compatible with standard PNA synthesis protocols for the Expedite 8909 DNA synthesizer. Starting from known intermediates **1a** and **1b** (Scheme 1),[16,18] reductive amination with Fmoc-glycinaldehyde[20]

Scheme 1. Synthesis of Fmoc-Protected GPNA Monomers[a]

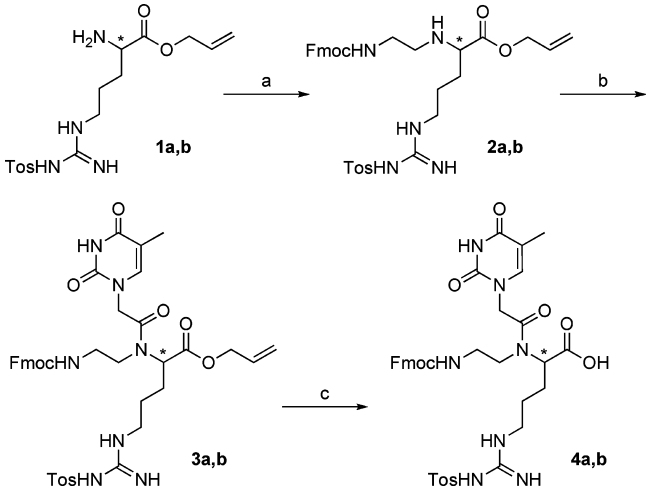

[a]The **a** series has *R* stereochemistry (derived from D-arginine) and the **b** series *S* stereochemistry (derived from L-arginine) at the chiral center (asterisks). Steps (yields for D-series): (a) Fmoc-$NHCH_2CHO$, MeOH, 0 °C, 4 h, acetic acid, $NaBH_3CN$, 30 min (57%); (b) thymine-1-acetic acid, 3-hydroxy-1,2,3-benzotriazin-4(3*H*)-one, *N*-[3-(dimethylamino)propyl]-*N*′-ethylcarbodiimide, dimethylformamide, 40 °C, 12 h (60%); (c) $Pd(PPh_3)_4$, *N*-ethylaniline, tetrahydrofuran, room temperature, 1 h (81%).

gave backbone intermediates **2a** and **2b**. The target thymidine GPNA monomers [**4a** and **4b** (Scheme 1)] were prepared by coupling of **2a** and **2b** with thymine-1-acetic acid, which was prepared according to established procedures,[18] followed by deprotection using *N*-ethylaniline and $Pd(PPh_3)_4$.[16,21]

The guanidine-modified PNA oligomers [GPNA (Figure 2)] were made using the standard Fmoc synthesis protocols on the Expedite 8909 synthesizer and purified by reverse-phase high-performance liquid chromatography. Cleavage from the solid support and removal of all protecting groups (including the *N*-tosyl group) were achieved with a mixture of *m*-cresol, thioanisole, trifluoromethanesulfonic acid, and trifluoroacetic acid (1:1:2:6) as previously reported.[16] To allow direct comparison, we prepared the same GPNA sequences (Figure 2), like the PNA used in our previous study of triple-helix formation with double-helical RNA.[10]

dx.doi.org/10.1021/bi201570a | *Biochemistry* 2012, 51, 63–73

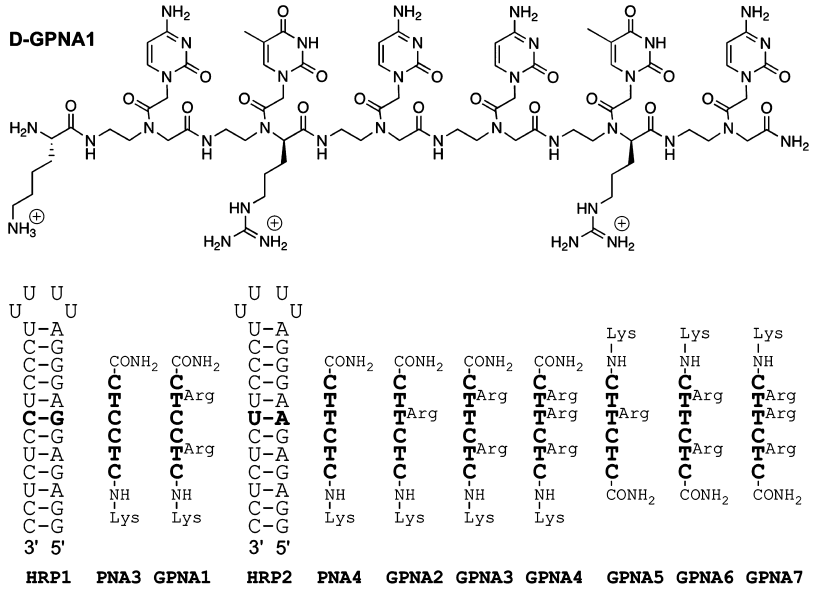

Figure 2. Structure of GPNA and sequences of RNA hairpins, PNA, and GPNA. The numbering of RNA hairpins and PNA is from ref 10.

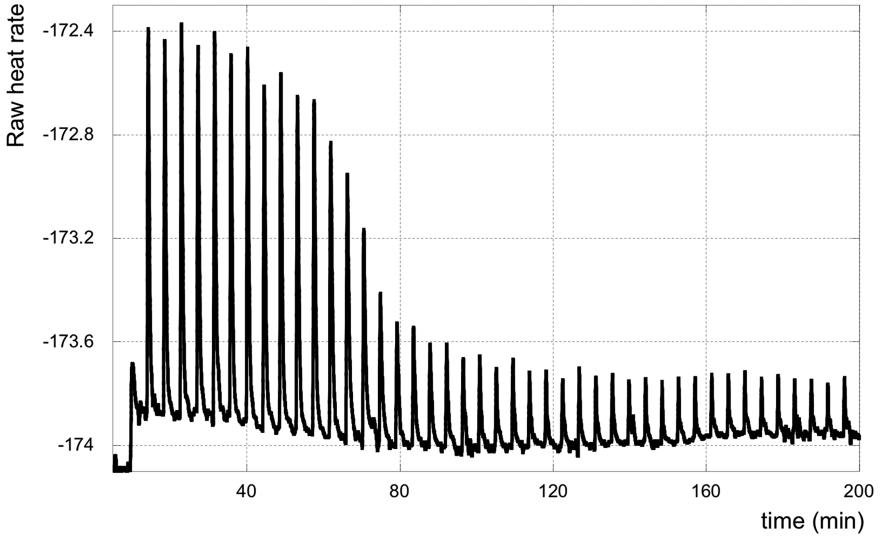

Figure 3. ITC titration curve of D-GPNA1 (5 μL injections of 96 μM) binding to HRP1 (5.25 μM).

The binding of GPNA to RNA hairpin (HRP1) was studied using isothermal titration calorimetry [ITC (Figure 3)].

The ITC results, summarized in Table 1, showed that modification of both T monomers in the hexamer CTCCTC (PNA3) with a guanidine residue derived from either D- or L-arginine lowered the affinity for double-stranded RNA (cf., entry 1 with entries 2 and 3). Interestingly, the binding order (PNA:RNA stoichiometry) increased from 1 (observed in our previous study) to 2, suggesting that a more complex binding mode, presumably a duplex invasion forming a GPNA–RNA–GPNA triple helix, was taking place (Figure 4). Formation of the complex was further confirmed using circular dichroism (CD) spectroscopy. Wittung et al. have shown that strand invasion of the DNA duplex by PNA resulted in a decrease in the magnitude of the CD signal at 240–250 nm and an increase in the magnitude of the CD signal at ~280 nm.[22,23] In contrast to unmodified PNA, GPNA exhibited a weak but notable CD signal (Figure 5A, blue and green lines) at the concentration used in ITC experiments. Addition of 4.5 equiv (conditions mimicking the end point of ITC titration) of D-GPNA1 and L-GPNA1 to HRP1 induced a decrease in the magnitude of the CD signal at 240–250 nm, which was clearly visible in the difference spectra (red lines in panels B and C of Figure 5, respectively). However, we did not observe a significant increase around 280 nm. In contrast, the binding of D-GPNA1 showed a decrease in the magnitude of the signal at that wavelength. Overall, the CD spectra confirmed the formation of GPNA–RNA complexes.

In accord with our previous study,[10] binding of D-GPNA1 to the HRP1 hairpin made of deoxynucleotides (DNA version of HRP1) was weaker by ~1 order of magnitude (cf., entries 2 and 4). In contrast, the affinity of L-GPNA1 for either the RNA or DNA hairpin was practically the same (cf., entries 3 and 5). Under physiologically relevant conditions [37 °C, in 2 mM $MgCl_2$, 90 mM KCl, 10 mM NaCl, and 50 mM potassium phosphate (pH 7.4)], we observed no binding of D-GPNA1 to HRP1.

The sequence of PNA3 was symmetric and thus provided optimal binding for formation of both a parallel triple helix and

dx.doi.org/10.1021/bi201570a | Biochemistry 2012, 51, 63–73

Table 1. Thermodynamic Data for Binding of PNA and GPNA to RNA and DNA Hairpins[a]

entry		sequence	K_a ($\times 10^6$ M^{-1})	$-\Delta H$ (kcal/mol)	$-\Delta S$ (eu)	$-\Delta G$ (kcal/mol)	binding order
		Symmetric Sequence, Optimal for a Parallel Triple Helix and an Antiparallel Duplex (strand invasion)					
1[b]	PNA3	NH_2-CTCCTC	84 ± 80	29.4 ± 5.3	63 ± 17	10.6 ± 0.5	1.1 ± 0.2
2	D-GPNA1	NH_2-CT$^{D\text{-}Arg}$CCT$^{D\text{-}Arg}$C	4.6 ± 1.6	27.3 ± 2.5	61 ± 9	9.1 ± 0.2	1.8 ± 0.1
3	L-GPNA1	NH_2-CT$^{L\text{-}Arg}$CCT$^{L\text{-}Arg}$C	2.2 ± 1.6	24.2 ± 9.6	53 ± 34	8.6 ± 0.5	2.0 ± 0.1
4[c]	D-GPNA1	NH_2-CT$^{D\text{-}Arg}$CCT$^{D\text{-}Arg}$C	0.4	29.1	72	7.7	2.1
5[c]	L-GPNA1	NH_2-CT$^{L\text{-}Arg}$CCT$^{L\text{-}Arg}$C	2.5	21.0	41	8.7	2.2
		Sequence Optimal for a Parallel Triple Helix					
6[b]	PNA4	NH_2-CTCTTC	47 ± 22	26.4 ± 3.2	54 ± 12	10.4 ± 0.3	1.3 ± 0.1
7	D-GPNA2	NH_2-CTCT$^{D\text{-}Arg}$TC	0.5	70.0	209	7.8	0.5
8	D-GPNA3	NH_2-CT$^{D\text{-}Arg}$CTT$^{D\text{-}Arg}$C	0.5	41.8	114	7.8	0.8
9	D-GPNA4	NH_2-CT$^{D\text{-}Arg}$CT$^{D\text{-}Arg}$T$^{D\text{-}Arg}$C	0.6	22.9	50	7.9	1.2
10	L-GPNA2	NH_2-CTCT$^{L\text{-}Arg}$TC	1.8	39.6	104	8.5	0.7
11	L-GPNA3	NH_2-CT$^{L\text{-}Arg}$CTT$^{L\text{-}Arg}$C	0.8	58.8	170	8.0	0.5
12	L-GPNA4	NH_2-CT$^{L\text{-}Arg}$CT$^{L\text{-}Arg}$T$^{L\text{-}Arg}$C	0.5	61.6	181	7.8	0.4
		Sequence Optimal for an Antiparallel Duplex (strand invasion)					
13[d]	D-GPNA5	NH_2-CTT$^{D\text{-}Arg}$CTC	10.5	19.8	34	9.6	1.4
14[d]	D-GPNA6	NH_2-CT$^{D\text{-}Arg}$TCT$^{D\text{-}Arg}$C	5.0	13.4	14	9.1	2.0
15[d]	D-GPNA7	NH_2-CT$^{D\text{-}Arg}$T$^{D\text{-}Arg}$CT$^{D\text{-}Arg}$C	0.4 ± 0.01	25.8 ± 3.7	61 ± 13	7.6 ± 0.0	2.3 ± 0.0
16[d]	L-GPNA7	NH_2-CT$^{L\text{-}Arg}$T$^{L\text{-}Arg}$CT$^{L\text{-}Arg}$C	3.8 ± 0.1	13.0 ± 7.3	14 ± 25	8.9 ± 0.3	2.1 ± 0.1

[a]Average association constants K_a (±standard deviation) in 100 mM sodium acetate and 1.0 mM EDTA (pH 5.5). Entries 1–3 are for binding to HRP1, entries 4 and 5 for binding to a DNA version of HRP1, and entries 6–16 for binding to HRP2. [b]From our previous study.[10] [c]Binding to a DNA version of HRP1. [d]PNA antiparallel to the purine tract of HRP2 (Figure 4B).

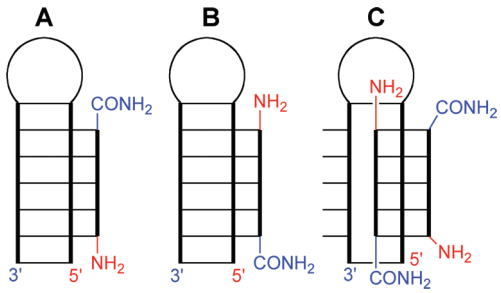

Figure 4. Schematic representation of the binding modes: (A) parallel triple helix (amino end of PNA aligned with the 5′ end of RNA), (B) antiparallel triple helix, and (C) strand invasion triplex that combines antiparallel PNA binding via Watson–Crick hydrogen bonds and parallel PNA binding via Hoogsteen hydrogen bonds.

an antiparallel duplex, as required for triplex invasion (Figure 4). To gain more insight into different binding modes, we prepared guanidine-modified variants of hexamer CTCTTC (PNA4) and studied their binding to HRP2. All the sequences designed to bind in a parallel mode to the polypurine tract of HRP2 [in GPNA2–GPNA4 (Figure 2), the amino terminus aligns with the 5′ end of RNA (see also Figure 4A)] had a similar affinity for the RNA target that was ~2 orders of magnitude lower than the affinity of the unmodified PNA4 (in Table 1, cf., entry 6 and entries 7–12). While there was very little dependence on the number of modifications in the D series (entries 7–9), in the L series (entries 10–12) the affinity appeared to decrease somewhat with an increasing number of guanidine modifications. Interestingly, increasing the number of modifications in the D series was followed by a decrease in both binding enthalpy and entropy (ΔH and ΔS, respectively, in Table 1), while the reverse was true in the L series. This result suggested that the stereoisomeric guanidine modifications had distinct interactions with the RNA target. The PNA:RNA stoichiometry (binding order in Table 1) suggested that the parallel GPNA maintained the original PNA–RNA–RNA triple-helical mode of recognition.

In contrast, the sequences designed to bind in an antiparallel mode (Figure 4B) to the polypurine tract of HRP2 [in GPNA5–GPNA7 (Figure 2), the amino terminus aligned with the 3′ end of RNA] had significant differences in binding affinity depending on the number and stereochemistry of guanidine modifications. In the D series (entries 13–15), the binding affinity decreased more than 20-fold going from one (entry 13) to three guanidine modifications (entry 15). The binding order increased to 2 with two and three guanidine modifications, suggesting that the antiparallel sequences may favor triplex invasion [GPNA–RNA–GPNA (Figure 4C)], as observed for GPNA1 (entries 2 and 3). GPNA7 derived from L-arginine (entry 16) had a significantly higher affinity than the D isomer (entry 15). Binding of GPNA7 to HRP2 produced similar changes in CD spectra as observed for GPNA1 and HRP1 (Figure S43 of the Supporting Information). While D-GPNA5 had the highest binding affinity [$K_a \sim 10^7$ (entry 13)] among all guanidine-modified PNA tested at pH 5.5, we observed no binding when the experiment in entry 13 was repeated in acetate buffer at pH 7.3.

Next we checked the sequence selectivity of binding of GPNA1 to all four RNA hairpins having a variable central base pair [HRP1–HRP4 (Figures 2 and 6)]. The results in Table 2 showed that the affinity of unmodified PNA3 and either the D or the L isomer of GPNA1 for the "mismatched" hairpins (HRP2–HRP4) was approximately the same (D-GPNA1 vs HRP4 was the only notable exception). Thus, the sequence specificity of GPNA was reduced compared to that of unmodified PNA because of the lower affinity for the "matched" target (highlighted in bold in Table 2). We also studied the sequence selectivity of antiparallel (Figure 4B) GPNA8 and GPNA9 in comparison with PNA5 and PNA6, respectively (Figure 6). These sequences all have a mismatched central Hoogsteen base triplet; however, because two molecules of D-GPNA8 and D-GPNA9 bind to an RNA hairpin [binding order of 2 (see the Supporting Information)], the combination D-GPNA8 and HRP3 and the combination of D-GPNA9 and

dx.doi.org/10.1021/bi201570a | Biochemistry 2012, 51, 63–73

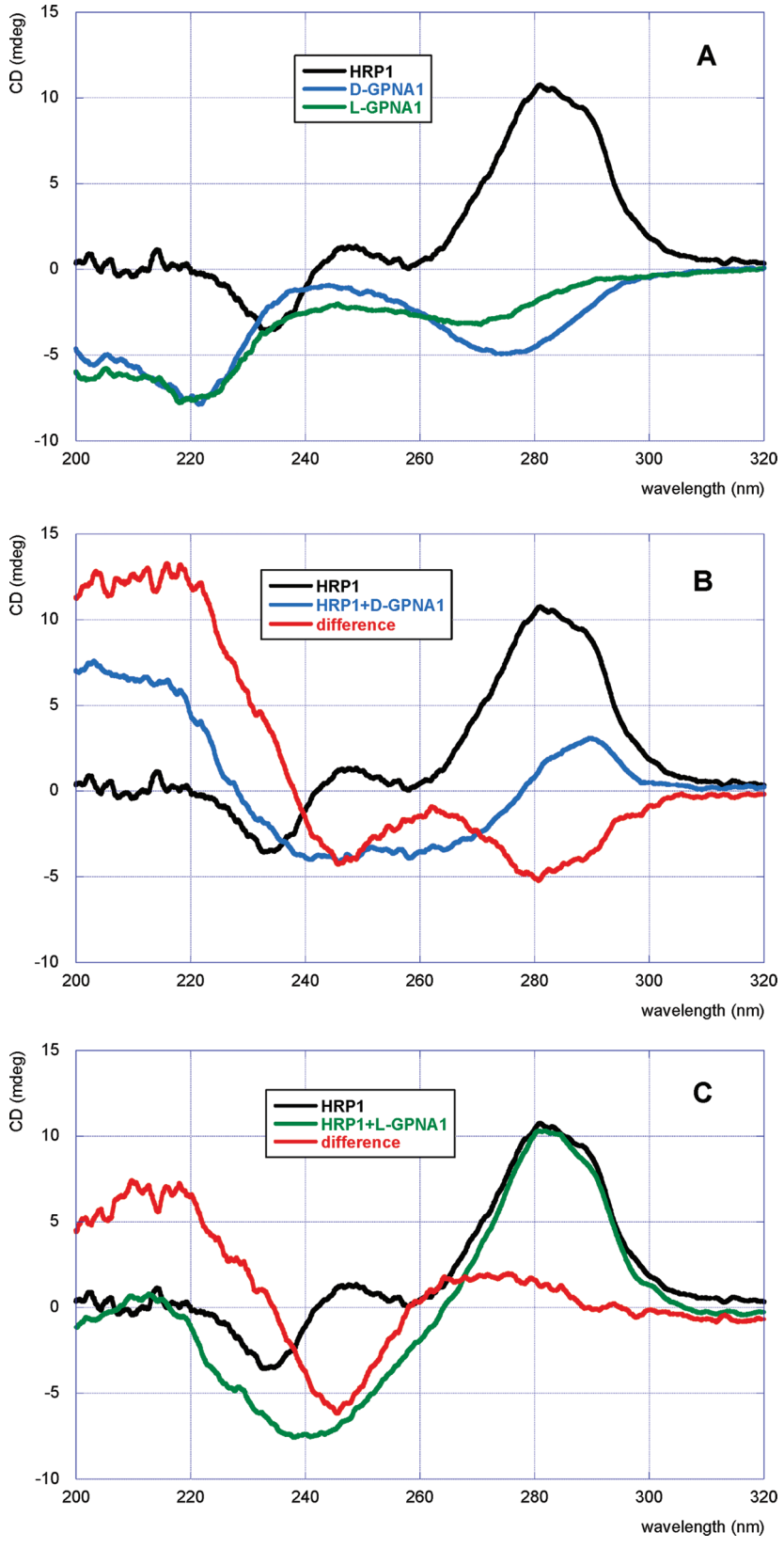

Figure 5. CD spectra of D-GPNA1, L-GPNA1, and HRP1 (A), binding of D-GPNA1 to HRP1 (B), and binding of L-GPNA1 to HRP1 (C). The red lines in panels B and C are the arithmetic difference between the complex spectra (GPNA + HRP1, blue and green in panels B and C, respectively) minus the sum of GPNA (blue and green in panel A) and HRP1 (black) spectra. The RNA concentration wass 5.25 μM, and the GPNA concentration was 24 μM.

HRP4 would have a matched Watson−Crick base pair if the binding were following the triplex-invasion mode (Figure 4C). Indeed, D-GPNA8 had a higher binding affinity than PNA5 for HRP3, consistent with formation of the G-C base pair upon

dx.doi.org/10.1021/bi201570a | *Biochemistry* 2012, 51, 63−73

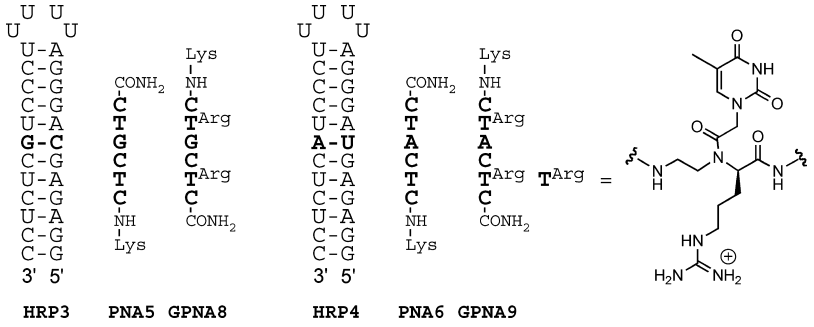

Figure 6. Structure of RNA hairpins, PNA, and GPNA used in our sequence selectivity study.

Table 2. Sequence Selectivity of Binding of GPNA to RNA Hairpins[a]

PNA (variable base)	HRP1[a] (G-C)	HRP2[a] (A-U)	HRP3[a] (C-G)	HRP4[a] (U-A)
PNA3 (C)[b]	**84**	0.4	0.5	0.2
D-GPNA1	**4.6**	0.3	0.7	1.3
L-GPNA1	**2.2**	0.8	0.6	0.4
PNA5 (G)[b]	1.5	0.4	**0.2**	**0.1**
D-GPNA8[c]	0.8	0.6	**1.2**	**0.7**
PNA6 (A)[b]	6.0	1.6	0.7	**0.05**
D-GPNA9[c]	ND[d]	0.6	ND[d]	**0.97**

[a]Average association constants [K_a ($\times 10^6$ M^{-1})] in sodium acetate buffer (pH 5.5). [b]From our previous study.[10] [c]PNA antiparallel to the purine tract of RNA. [d]Not determined.

invasion, and HRP4, possibly due to a stabilizing G-U wobble base pair (highlighted in bold in Table 2). A similar result, consistent with formation of an A-U base pair, was obtained for the combination of D-GPNA9 and HRP4, supporting our hypothesis that the binding order of 2 indicated triplex invasion and formation of a GPNA−RNA−GPNA complex.

Next, we tested if PNA and GPNA could recognize more complex biologically relevant RNA, such as the ribosomal A-site. Model hairpins (Figure 7) were designed to contain the secondary structure of ribosomal A-sites (sequences from http://www.rna.ccbb.utexas.edu/) of *Homo sapiens* (HRP5) and *Mycobacterium tuberculosis* (HRP6) and to close at one end with a stable RNA tetraloop and on the other end with a couple of C-G base pairs. The structures of the A-rich bulge, which is the target of aminoglycoside antibiotics, of bacterial and human A-sites are remarkably similar. However, significant differences occur in the helical region just above the A-rich bulge (bold in Figure 7). Interestingly, the A-site helices feature short polypurine tracts interrupted by a single pyrimidine, U in HRP5 and C in HRP6, which prompted us to explore if the A-site RNA may be recognized via triplex or triplex-invasion mode (Figure 7 and Table 3).

Table 3. Binding of PNA and GPNA (L series) to Ribosomal A-Site Model RNA Hairpins (Figure 7)[a]

entry	PNA	sequence	*M. tuberculosis* (HRP6)	*H. sapiens* (HRP5)
1	PNA10	NH_2-CCCTGCTT	1.2 (1.7)	0.4 (2.0)
2	GPNA10	NH_2-CCCT$^{L\text{-}Arg}$GCT$^{L\text{-}Arg}$T	0.5 (2.9)	2.8 (5.0)
3	PNA11	NH_2-CCTGCTT	0.2 (1.1)	0.04 (0.9)
4	PNA12	NH_2-CTGCTT	0.2 (1.6)	0.06 (0.9)
5	GPNA12	NH_2-CT$^{L\text{-}Arg}$GCTT	0.4 (1.8)	0.8 (2.1)
6	GPNA13	NH_2-CT$^{L\text{-}Arg}$GCT$^{L\text{-}Arg}$T	2.9 (8.0)	8.1 (8.8)
7	PNA13	NH_2-CCCTPCTT	1.5 (1.1)	NB[b]
8	PNA14	NH_2-CCCTP$_{ex}$CTT	2.0 (1.1)	NB[b]

[a]Average association constants [K_a ($\times 10^6$ M^{-1})] in sodium acetate buffer (pH 5.5); the binding order is given in parentheses. [b]No binding; $K_a < 10^3$ M^{-1}.

In general, PNA and GPNA (L series) targeting the A-site exhibited modest binding affinity, which was consistent with the impact of a mismatched base triplet observed in our previous study.[10] Octamer PNA10 had low sequence selectivity for the bacterial A-site, and the binding order indicated potential triplex invasion (Table 3, entry 1). Surprisingly, guanidine modification resulted in an increased affinity of GPNA10 for the human A-site and a dramatic loss of sequence selectivity, which correlated with large increases in the level of

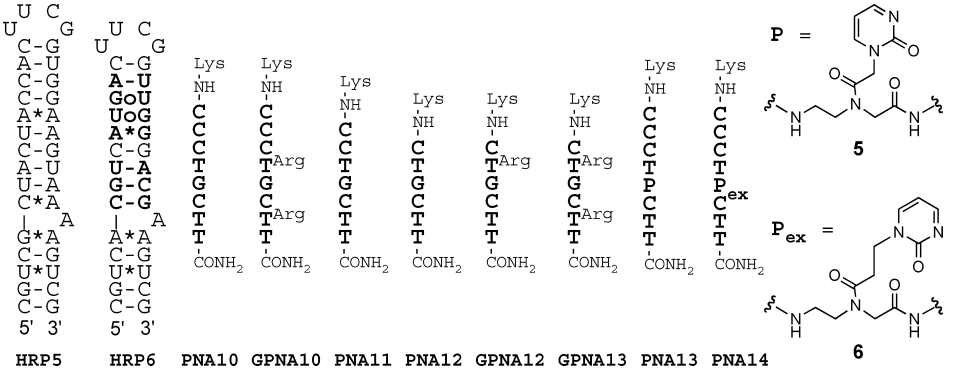

Figure 7. Structure of ribosomal A-site model RNA hairpins and the complementary PNA and GPNA.

dx.doi.org/10.1021/bi201570a | *Biochemistry* 2012, 51, 63−73

binding order (Table 3, entry 2). Shortening the PNA to a heptamer (PNA11) and a hexamer (PNA12) slightly decreased the affinity and increased the sequence selectivity. Guanidine modifications in GPNA12 and GPNA13 increased the binding affinity, but the sequence selectivity was lost. It is conceivable that the unusually high binding orders for GPNA10 and GPNA13 resulted from nonspecific electrostatic association of these GPNA carrying two guanidine modifications with the relatively more flexible (because of the noncanonical base pairs) A-site RNA. Recently, we showed that 2-pyrimidone, as in the novel PNA monomers **5** and **6** (Figure 7) formed a matched triplet with a C-G inversion in the purine-rich strand of double-helical RNA.[12] Replacing the mismatched G in PNA10 with P and P_{ex} (monomers **5** and **6**, respectively) increased the affinity of PNA13 and PNA14 for the bacterial A-site. The stoichiometry of the complex was close to 1:1 as expected for the triple helix. Most remarkably, the sequence selectivity was excellent; we could not observe any binding to the human A-site (Figures S40 and S42 of the Supporting Information).

The preference of guanidine-modified PNA to form strand invasion complexes prompted us to check if GPNA could bind RNA structures that do not have continuous polypurine tracts. To test this hypothesis, we selected a model RNA sequence of the transactivation response element (TAR) of HIV-1 virus (Figure 8). We envisioned that the bulged structure should be

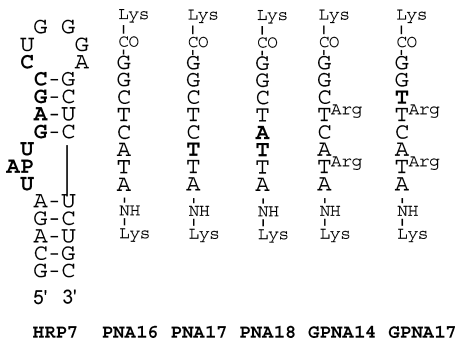

Figure 8. Structure of the TAR RNA hairpin and complementary PNA and GPNA. The target site on RNA and the mismatched nucleobases are highlighted in bold; AP is 2-aminopurine.

thermally less stable than a canonical Watson–Crick helix and may predispose the RNA for strand invasion by PNA. To test this hypothesis, we chose PNA16 complementary to the U-rich loop and the stem connecting the U-rich loop and the hairpin loop. This sequence design was similar to that of Pandey[24–26] and others,[27] except that we decided not to include the G-rich hairpin loop in the recognition site because our focus was on testing duplex invasion as opposed to Watson–Crick binding to the flexible loop. Our initial experiments were frustrated by an apparent aggregation of PNA at high concentrations (~100 μM) in the injection syringe of ITC. While PNA used in the ITC studies described above had no more than one purine base (<20%), PNA complementary to TAR RNA had 50% purines (Figure 8), which may cause some aggregation at high concentrations. In a search for an alternative method, we turned to fluorescence spectroscopy of RNA labeled with the highly fluorescent 2-aminopurine nucleoside.[19,28–30] 2-Aminopurine fluorescence has been used to characterize binding of small molecules to the rev responsive element RNA of HIV-1,[28] aminoglycosides to the ribosomal A-site,[29,30] and, most recently, argininamide, Tat peptide, and neomycin to TAR RNA model construct HRP7[19] (Figure 8).

Following the published methodology,[19] incremental titration of HRP7 with PNA16 led to a decrease in fluorescence intensity (red circles in Figure 9A), as expected for 2-aminopurine moving from a relatively flexible bulge to a more structured PNA–RNA duplex environment. Fitting the data (Figure S44 of the Supporting Information) to a single site, two-state binding model gave a K_a of ~2×10^7 M^{-1}.[19] Introduction of a mismatch (highlighted in bold in Figure 8) lowered the affinity of PNA17 (blue squares in Figure 9A) to ~4×10^6 M^{-1}. Two adjacent mismatches in PNA18 led to a curve (green triangles in Figure 9A) that fit poorly the single-site, two-state binding model (Figure S46 of the Supporting Information); however, the relatively small slope clearly indicated a significantly decreased affinity. Binding of L-GPNA14 to HRP7 appeared to be weaker than that of unmodified PNA16 (Figure 9B). The curve did not fit well the single-site, two-state binding model (Figure S47 of the Supporting Information), giving a K_a of approximately $2–5 \times 10^6$ M^{-1}, which was comparable to that of PNA17 having a mismatched base pair. Surprisingly, introduction of a mismatch did not significantly change the affinity of L-GPNA17 (Figure 9B; see also Figures S47 and S48 of the Supporting Information). This result might indicate that a significant portion of the binding energy came from nonspecific electrostatic attraction. In contrast, D-GPNA14 had an apparently higher affinity for HRP7 than the unmodified PNA16 (blue squares in Figure 9C). Fitting the data (Figure S49 of the Supporting Information) to a single-site, two-state binding model gave a K_a of ~10^8 M^{-1}.[19] Introduction of a mismatch lowered the affinity of D-GPNA17 (green triangles in Figure 9C). The curve did not fit well the single-site, two-state binding model (Figure S50 of the Supporting Information), giving a K_a of approximately 2×10^6 M^{-1}, which was comparable to that of the mismatched PNA17 and L-GPNA17. One potential explanation for the poor fitting of data for mismatched PNA18, L-GPNA, and D-GPNA17 is that more than 1 equivalent of PNA was binding to HRP7, causing significant deviations from the single-site, two-state binding model behavior.

Formation of the complex between the TAR RNA model hairpin and PNA was further confirmed using a gel mobility shift assay (Figure 10). Incremental titration of HRP7 (5′-labeled with fluorescein) with PNA16 (Figure 10A) and D-GPNA14 (Figure 10B) led to the disappearance of the RNA band and formation of a slower-moving band, which could be assigned to a potential strand invasion complex.[27,31] Interestingly and in contrast to PNA16, addition of >2 equiv of D-GPNA14 led to the disappearance of the initial complex band and formation of broad and smeared out bands that were diluted below the detection level. This result suggested that >1 equiv of guanidine-modified PNA may be binding to HRP7 with a lower affinity at higher PNA:RNA ratios.

DISCUSSION

PNA bearing cationic α- and γ-substituents bind strongly to cDNA and RNA and exhibit interesting biological properties.[16–18,32–34] Ly and co-workers[16–18] have reported that guanidine modification of PNA greatly facilitates the traversal of the cellular membrane, a highly desirable property for in vivo applications of gene expression control. They found that GPNA induced a potent and sequence specific antisense effect and was less toxic to the cells compared to PNA conjugated with polyarginine.[32] These favorable properties prompted us to study binding of GPNA to double-helical RNA, especially because we had recently discovered that unmodified

dx.doi.org/10.1021/bi201570a | Biochemistry 2012, 51, 63–73

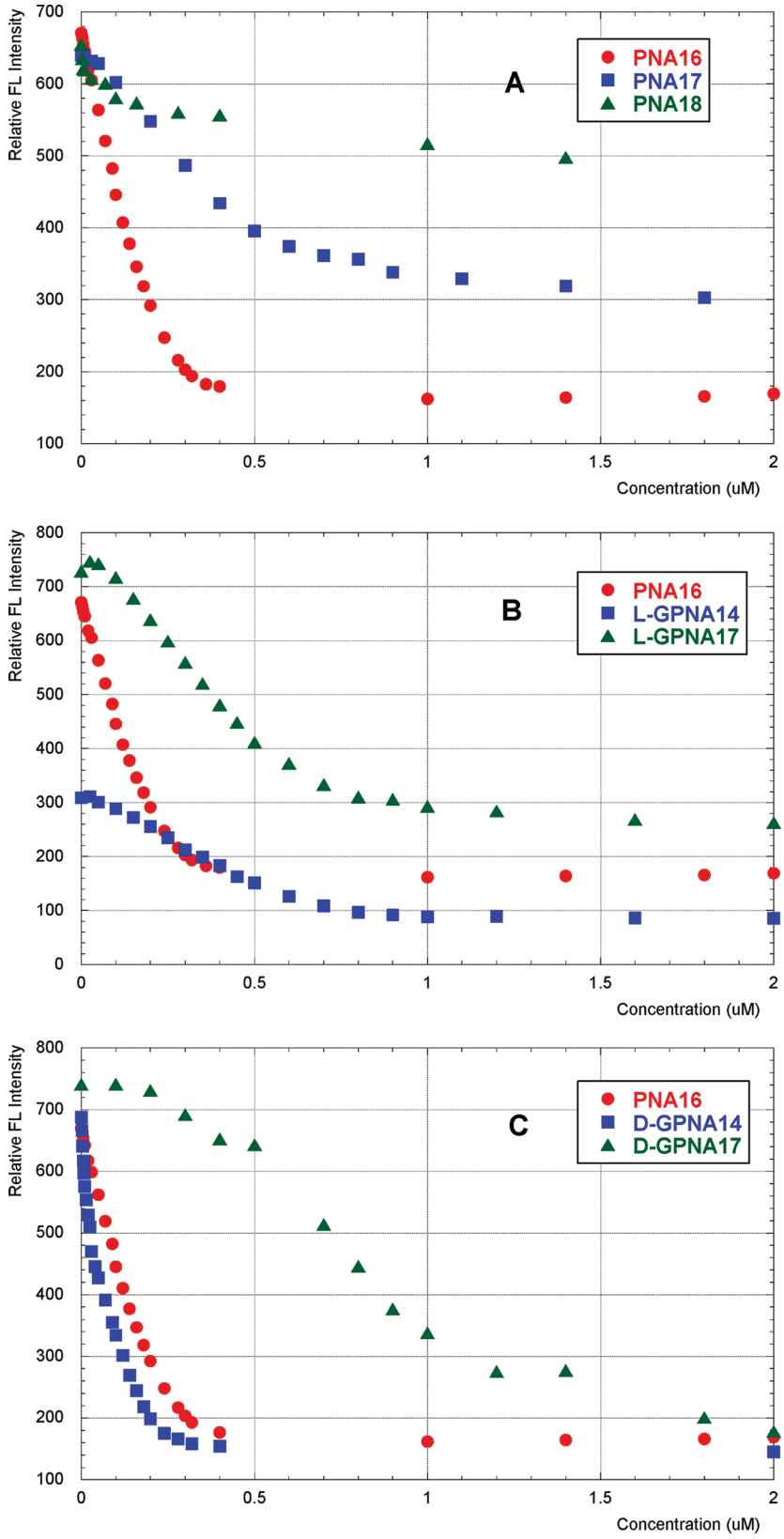

Figure 9. Binding of PNA and GPNA to TAR RNA HRP7. The change in fluorescence was monitored at 365 nm following excitation at 305 nm.

PNA bind surprisingly strongly and sequence selectively to double-helical RNA.[10−12]

Ly and co-workers demonstrated that L-GPNA had a lower affinity for complementary single-stranded DNA[16] and RNA[17] than unmodified PNA. In contrast, the affinity of D-GPNA was similar or even higher than that of unmodified PNA.[16,17] In our hands, both isomers of GPNA sequences optimized for parallel binding to the polypurine tract of double-helical RNA had

dx.doi.org/10.1021/bi201570a | *Biochemistry* 2012, 51, 63−73

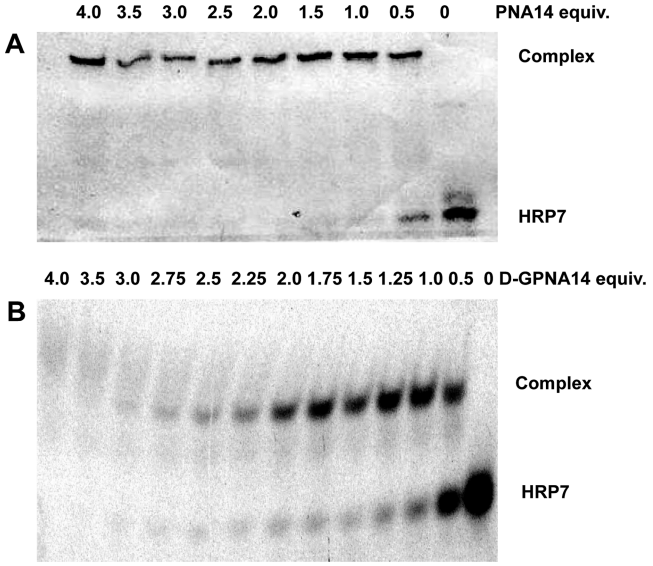

Figure 10. Binding of PNA16 (A) and D-GPNA14 (B) to 5′-fluorescein-labeled TAR RNA HRP7 (5 μM) monitored by a gel mobility shift assay. Gels were run in 89 mM tris-borate buffer and 2 mM EDTA (pH 8.4).

binding affinities ~2 orders of magnitude lower than that of the unmodified PNA (cf., Table 1, entry 6 and entries 7−12). This result suggested that a PNA backbone derived from α-substituted amino acids instead of glycine might be a poor fit for the PNA−RNA−RNA triple helix. The problem is most likely steric hindrance because the cationic guanidine modification could be expected to enhance the stability of triple helices at the expense of sequence selectivity. For example, conjugation of cationic peptides at PNA termini has been shown to increase the stability of PNA−DNA−DNA triple helices.[31] Interestingly, Ly and co-workers[18] found that GPNA T_{10} formed a GPNA−DNA duplex but not a GPNA−DNA−GPNA triplex with the complementary dA_{10}, a result consistent with our findings that the guanidine modification disfavors triple-helix formation.

GPNA sequences optimized for antiparallel binding to the polypurine tract had somewhat higher affinities for double-helical RNA than the parallel GPNA sequences ($K_a = 10^6-10^7$, depending on the sequence and number of modifications). However, the affinity was lower than that of unmodified PNA and decreased with an increasing number of guanidine modifications (Table 1, entries 13−15). Multiple modifications derived from L-arginine appeared to be better tolerated, leading to a higher affinity of L-GPNA (Table 1, entry 16) than D-GPNA (entry 15). This was somewhat unexpected because D-GPNA were shown to form more stable duplexes with DNA and RNA than L-GPNA.[16,17] However, if the antiparallel GPNA bind RNA by triplex invasion, both the favored antiparallel GPNA−RNA duplex and the antiparallel GPNA−RNA−GPNA triple helix (see Figure 4) contribute to the overall stability of the complex. We recently showed that unmodified PNA formed both parallel and antiparallel triple helices with RNA (Figure 4A,B), though the latter was 1 order of magnitude less stable.[10] It is conceivable that the antiparallel triple helix is disfavored more by the D modification than by the L modification.

For the symmetric sequence CTCCTC, which was optimal for both the parallel triple helix and the antiparallel duplex (as required for triplex invasion), we observed an overall decrease in binding affinity upon guanidine modification (Table 1, entries 1−3). Consistent with more stable duplexes involving D-GPNA[17] and equally destabilized parallel triple helices (Table 1, entries 6−12), D-GPNA1 had a slightly higher affinity than L-GPNA1 (cf., entries 2 and 3). Perhaps the most interesting finding was that guanidine modification shifted the binding mode from 1:1 (as indicated by a binding stoichiometry of ~1), which we assign to the GPNA−RNA−RNA triplex, to 2:1 (binding stoichiometry of ~2). We propose that the best explanation for the 2:1 complex is a GPNA−RNA−GPNA triplex invasion complex (Figure 4C). The relatively higher stability of GPNA−RNA complexes that can form Watson−Crick base pairs (D-GPNA8 with HRP3 and D-GPNA9 with HRP4) or G-U wobble pair supports our hypothesis of triplex invasion. Thus, guanidine modification of PNA at the α-position appears to enhance the strand invasion of the RNA double helix, which is consistent with observations made by others that cationic modifications and α- and γ-substituents predispose PNA for strand invasion of DNA.[24,25,35−37] Our experiments with TAR RNA model HRP7 further confirmed that guanidine modification promotes RNA strand invasion. The fact that D-GPNA14 had a significantly higher affinity and sequence selectivity than L-GPNA14 was encouraging for future applications and fully consistent with previous findings by Ly and co-workers.[16,17] Overall, the guanidine modification significantly weakened the ability of PNA to form triple helices with complementary double-helical RNA. Meanwhile, the affinity of GPNA and unmodified PNA for mismatched RNA helices was lowered by approximately the same extent (Table 2), which resulted in an overall decrease in sequence selectivity for GPNA.

Binding of PNA to A-site RNA had not been studied prior to our recent work.[12] Our results show that unmodified PNA were able to bind the polypurine tract of bacterial A-site RNA in preference to human A-site RNA. The relatively low affinity and modest sequence selectivity of binding were most likely due to the inability of Hoogsteen triplets to recognize the pyrimidine interruption in the polypurine tract of HRP6. The results with PNA11 and PNA12 are encouraging for triplex recognition of A-site RNA, providing that a modified heterocycle could be designed that would recognize the pyrimidine interruption in the polypurine tract and restore binding affinity and sequence selectivity.[38−40] Consistent with this notion, incorporation of modified heterocyles [P and P_{ex} (Figure 7)], recently developed by us to recognize cytosine in G-C inversion,[12] significantly increased the sequence selectivity while maintaining excellent affinity in the triple-helical binding mode (Table 3). A brief review of secondary structure databases of noncoding RNAs reveals that it is relatively common to find short homopurine tracts of eight and more contiguous purines, sometimes interrupted by one or two pyrimidines, in bacterial rRNAs (http://www.rna.ccbb.utexas.edu/) and micro RNAs (http://www.mirbase.org/). Our preliminary results with PNA13 and PNA14 suggest the possibility of designing relatively small PNA analogues to recognize such binding sites. It is conceivable that further development of chemical modifications may allow general recognition of isolated pyrimidines in the context of the homopurine triple helix at physiological pH, which may open a novel way to recognize and interfere with function of noncoding RNAs.

Because of the need for cytosine ($pK_a \sim 4.5$) protonation to form the Hoogsteen C*G-C triplets, the experiments on triple-helical recognition of RNA were performed at pH 5.5. Consistent

dx.doi.org/10.1021/bi201570a | Biochemistry 2012, 51, 63−73

with this requirement, we did not observe binding of GPNA to RNA hairpins at physiologically relevant pH values. This problem is beyond the scope of this work and may be addressed in future work by designing PNA containing more basic cytosine analogues and/or alternative cationic modifications.[31] While the α-guanidine-modified PNA did not improve triple-helix formation with double-helical RNA, related cationic modifications, such as PNA modified with γ-guanidine[34] and γ-lysine,[33] still are interesting alternatives, which may allow effective triple-helical recognition and enhanced cellular uptake to be realized in a modified PNA analogue.

A promising result was obtained using D-GPNA14 in a strand invasion mode with the TAR RNA hairpin. Binding of PNA to TAR RNA has previously been demonstrated by gel mobility shift analysis and by blocking the Tat-mediated transactivation in a cell culture.[26,27] The data are consistent with formation of a 1:1 PNA−RNA strand invasion duplex.[26,27] Similarly, PNA14 and especially D-GPNA14 showed excellent affinity and sequence selectivity for TAR RNA. The gel mobility shift assay and a good fit of the fluorescence data to a single-site, two-state binding model suggested formation of a 1:1 PNA−RNA complex, most likely a strand invasion duplex, as previously reported by others.[27] However, gel mobility experiments also indicated that guanidine modifications may cause nonselective binding of additional PNA molecules to the RNA hairpin at higher concentrations. Consistent with the literature data,[16,17] guanidine modification in L-GPNA14 decreased the binding affinity and sequence selectivity. Overall, D-GPNA may be promising compounds to explore for strand invasion recognition of biologically relevant RNAs featuring hairpin structures that are thermally weaker because of noncanonical base pairs, bulges, and internal loops. Finally, it should be noted that this study was conducted on relatively short (hexamer to octamer) PNA. It is conceivable that longer PNA will be required to recognize the target RNA sequences selectively in the presence of other DNA and RNA species in cells. Such studies will be a future priority after strong binding at physiologically relevant conditions is achieved by additional chemical modifications.

■ ASSOCIATED CONTENT

Supporting Information

Details of PNA synthesis, ITC experiments and data, CD spectra, fitting of fluorescence data, and copies of NMR spectra. This material is available free of charge via the Internet at http://pubs.acs.org.

■ AUTHOR INFORMATION

Corresponding Author

*Department of Chemistry, Binghamton University, The State University of New York, Binghamton, NY 13902. Telephone: (607) 777-2441. Fax: (607) 777-4478. E-mail: erozners@binghamton.edu.

Funding

We thank the National Institutes of Health (R01 GM071461), Binghamton University, and the Clifford D. Clark Graduate Fellowship (to O.M.) for financial support of this research.

■ ACKNOWLEDGMENTS

We thank Prof. Susannah Gal (Biological Sciences, Binghamton University) for help with the gel mobility shift assay.

■ REFERENCES

(1) Thomas, J. R., and Hergenrother, P. J. (2008) Targeting RNA with Small Molecules. *Chem. Rev. 108*, 1171−1224.
(2) Sucheck, S. J., and Wong, C. H. (2000) RNA as a target for small molecules. *Curr. Opin. Chem. Biol. 4*, 678−686.
(3) Chow, C. S., and Bogdan, F. M. (1997) A Structural Basis for RNA-Ligand Interactions. *Chem. Rev. 97*, 1489−1513.
(4) Fox, K. R., and Brown, T. (2005) An extra dimension in nucleic acid sequence recognition. *Q. Rev. Biophys. 38*, 311−320.
(5) Roberts, R. W., and Crothers, D. M. (1992) Stability and properties of double and triple helices: Dramatic effects of RNA or DNA backbone composition. *Science 258*, 1463−1466.
(6) Han, H., and Dervan, P. B. (1993) Sequence-specific recognition of double helical RNA and RNA-DNA by triple helix formation. *Proc. Natl. Acad. Sci. U.S.A. 90*, 3806−3810.
(7) Escude, C., Francois, J. C., Sun, J. S., Ott, G., Sprinzl, M., Garestier, T., and Helene, C. (1993) Stability of triple helixes containing RNA and DNA strands: Experimental and molecular modeling studies. *Nucleic Acids Res. 21*, 5547−5553.
(8) Semerad, C. L., and Maher, L. J. III (1994) Exclusion of RNA strands from a purine motif triple helix. *Nucleic Acids Res. 22*, 5321−5325.
(9) Nielsen, P. E., Egholm, M., Berg, R. H., and Buchardt, O. (1991) Sequence-selective recognition of DNA by strand displacement with a thymine-substituted polyamide. *Science 254*, 1497−1500.
(10) Li, M., Zengeya, T., and Rozners, E. (2010) Short Peptide Nucleic Acids Bind Strongly to Homopurine Tract of Double Helical RNA at pH 5.5. *J. Am. Chem. Soc. 132*, 8676−8681.
(11) Zengeya, T., Li, M., and Rozners, E. (2011) PNA containing isocytidine nucleobase: Synthesis and recognition of double helical RNA. *Bioorg. Med. Chem. Lett. 21*, 2121−2124.
(12) Gupta, P., Zengeya, T., and Rozners, E. (2011) Triple helical recognition of pyrimidine inversions in polypurine tracts of RNA by nucleobase-modified PNA. *Chem. Commun. 47*, 11125−11127.
(13) Nielsen, P. E. (2010) Sequence-selective targeting of duplex DNA by peptide nucleic acids. *Curr. Opin. Mol. Ther. 12*, 184−191.
(14) Shiraishi, T., and Nielsen, P. E. (2006) Enhanced delivery of cell-penetrating peptide-peptide nucleic acid conjugates by endosomal disruption. *Nat. Protoc. 1*, 633−636.
(15) Nielsen, P. E. (2005) Addressing the challenges of cellular delivery and bioavailability of peptide nucleic acids (PNA). *Q. Rev. Biotech. 38*, 345−350.
(16) Zhou, P., Dragulescu-Andrasi, A., Bhattacharya, B., O'Keefe, H., Vatta, P., Hyldig-Nielsen, J. J., and Ly, D. H. (2006) Synthesis of cell-permeable peptide nucleic acids and characterization of their hybridization and uptake properties. *Bioorg. Med. Chem. Lett. 16*, 4931−4935.
(17) Dragulescu-Andrasi, A., Zhou, P., He, G., and Ly, D. H. (2005) Cell-permeable GPNA with appropriate backbone stereochemistry and spacing binds sequence-specifically to RNA. *Chem. Commun.*, 244−246.
(18) Zhou, P., Wang, M., Du, L., Fisher, G. W., Waggoner, A., and Ly, D. H. (2003) Novel Binding and Efficient Cellular Uptake of Guanidine-Based Peptide Nucleic Acids (GPNA). *J. Am. Chem. Soc. 125*, 6878−6879.
(19) Bradrick, T. D., and Marino, J. P. (2004) Ligand-induced changes in 2-aminopurine fluorescence as a probe for small molecule binding to HIV-1 TAR RNA. *RNA 10*, 1459−1468.
(20) Wojciechowski, F., and Hudson, R. H. E. (2008) A Convenient Route to N-[2-(Fmoc)aminoethyl]glycine Esters and PNA Oligomerization Using a Bis-N-Boc Nucleobase Protecting Group Strategy. *J. Org. Chem. 73*, 3807−3816.
(21) Kleiner, R. E., Brudno, Y., Birnbaum, M. E., and Liu, D. R. (2008) DNA-Templated Polymerization of Side-Chain-Functionalized Peptide Nucleic Acid Aldehydes. *J. Am. Chem. Soc. 130*, 4646−4659.
(22) Wittung, P., Nielsen, P., and Norden, B. (1996) Direct Observation of Strand Invasion by Peptide Nucleic Acid (PNA) into Double-Stranded DNA. *J. Am. Chem. Soc. 118*, 7049−7054.

(23) Wittung, P., Nielsen, P., and Norden, B. (1997) Extended DNA-recognition repertoire of peptide nucleic acid (PNA): PNA-dsDNA triplex formed with cytosine-rich homopyrimidine PNA. *Biochemistry 36*, 7973−7979.
(24) Kaushik, N., Basu, A., Palumbo, P., Myers, R. L., and Pandey, V. N. (2002) Anti-TAR polyamide nucleotide analog conjugated with a membrane-permeating peptide inhibits human immunodeficiency virus type 1 production. *J. Virol. 76*, 3881−3891.
(25) Tripathi, S., Chaubey, B., Ganguly, S., Harris, D., Casale, R. A., and Pandey, V. N. (2005) Anti-HIV-1 activity of anti-TAR polyamide nucleic acid conjugated with various membrane transducing peptides. *Nucleic Acids Res. 33*, 4345−4356.
(26) Mayhood, T., Kaushik, N., Pandey, P. K., Kashanchi, F., Deng, L., and Pandey, V. N. (2000) Inhibition of Tat-Mediated Transactivation of HIV-1 LTR Transcription by Polyamide Nucleic Acid Targeted to TAR Hairpin Element. *Biochemistry 39*, 11532−11539.
(27) Belousoff, M. J., Gasser, G., Graham, B., Tor, Y., and Spiccia, L. (2009) Binding of HIV-1 TAR mRNA to a peptide nucleic acid oligomer and its conjugates with metal-ion-binding multidentate ligands. *J. Biol. Inorg. Chem. 14*, 287−300.
(28) Lacourciere, K. A., Stivers, J. T., and Marino, J. P. (2000) Mechanism of Neomycin and Rev Peptide Binding to the Rev Responsive Element of HIV-1 As Determined by Fluorescence and NMR Spectroscopy. *Biochemistry 39*, 5630−5641.
(29) Kaul, M., Barbieri, C. M., and Pilch, D. S. (2004) Fluorescence-Based Approach for Detecting and Characterizing Antibiotic-Induced Conformational Changes in Ribosomal RNA: Comparing Aminoglycoside Binding to Prokaryotic and Eukaryotic Ribosomal RNA Sequences. *J. Am. Chem. Soc. 126*, 3447−3453.
(30) Blount, K. F., Zhao, F., Hermann, T., and Tor, Y. (2005) Conformational Constraint as a Means for Understanding RNA-Aminoglycoside Specificity. *J. Am. Chem. Soc. 127*, 9818−9829.
(31) Hansen, M. E., Bentin, T., and Nielsen, P. E. (2009) High-affinity triplex targeting of double stranded DNA using chemically modified peptide nucleic acid oligomers. *Nucleic Acids Res. 37*, 4498−4507.
(32) Dragulescu-Andrasi, A., Rapireddy, S., He, G., Bhattacharya, B., Hyldig-Nielsen, J. J., Zon, G., and Ly, D. H. (2006) Cell-Permeable Peptide Nucleic Acid Designed to Bind to the 5′-Untranslated Region of E-cadherin Transcript Induces Potent and Sequence-Specific Antisense Effects. *J. Am. Chem. Soc. 128*, 16104−16112.
(33) Englund, E. A., and Appella, D. H. (2007) γ-substituted peptide nucleic acids constructed from L-lysine are a versatile scaffold for multifunctional display. *Angew. Chem., Int. Ed. 46*, 1414−1418.
(34) Sahu, B., Chenna, V., Lathrop, K. L., Thomas, S. M., Zon, G., Livak, K. J., and Ly, D. H. (2009) Synthesis of Conformationally Preorganized and Cell-Permeable Guanidine-Based γ-Peptide Nucleic Acids (γ-GPNAs). *J. Org. Chem. 74*, 1509−1516.
(35) Ishizuka, T., Tedeschi, T., Corradini, R., Komiyama, M., Sforza, S., and Marchelli, R. (2009) SSB-Assisted Duplex Invasion of Preorganized PNA into Double-Stranded DNA. *ChemBioChem 10*, 2607−2612.
(36) He, G., Rapireddy, S., Bahal, R., Sahu, B., and Ly, D. H. (2009) Strand Invasion of Extended, Mixed-Sequence B-DNA by γ-PNAs. *J. Am. Chem. Soc. 131*, 12088−12090.
(37) Kaihatsu, K., Braasch, D. A., Cansizoglu, A., and Corey, D. R. (2002) Enhanced strand invasion by peptide nucleic acid-peptide conjugates. *Biochemistry 41*, 11118−11125.
(38) Rusling, D. A., Broughton-Head, V. J., Brown, T., and Fox, K. R. (2008) Towards the targeted modulation of gene expression by modified triplex-forming oligonucleotides. *Curr. Chem. Biol. 2*, 1−10.
(39) Rusling, D. A., Powers, V. E. C., Ranasinghe, R. T., Wang, Y., Osborne, S. D., Brown, T., and Fox, K. R. (2005) Four base recognition by triplex-forming oligonucleotides at physiological pH. *Nucleic Acids Res. 33*, 3025−3032.
(40) Buchini, S., and Leumann, C. J. (2003) Recent improvements in antigene technology. *Curr. Opin. Chem. Biol. 7*, 717−726.